

Title	Study of electron and proton isochoric heating for fast ignition
Author(s)	Key, M.H.; Akli, K.; Beg, F.; Chen, M.H.; Chung, H.-K.; Freeman, R.R.; Foord, M.E.; Green, J.S.; Gu, P.; Gregori, G.; Habara, H.; Hatchett, S.P.; Hey, D.; Hill, J.M.; King, J.A.; Kodama, R.; Koch, J.A.; Lancaster, K.; Lasinski, B.F.; Langdon, B.; MacKinnon, A.J.; Murphy, C.D.; Norreys, P.A.; Patel, N.; Patel, P.; Pasley, J.; Snavely, R.A.; Stephens, R.B.; Stoeckl, C.; Tabak, M.; Theobald, W.; Tanaka, K.; Town, R.; Wilks, S.C.; Yabuuchi, T.; Zhang, B.
Citation	Journal De Physique. IV : JP. 133 P.371-P.378
Issue Date	2006-06
Text Version	publisher
URL	<a href="http://hdl.handle.net/11094/3420">http://hdl.handle.net/11094/3420</a>
DOI	10.1051/jp4:2006133075
rights	
Note	

*Osaka University Knowledge Archive : OUKA*

<https://ir.library.osaka-u.ac.jp/>

Osaka University

## Study of electron and proton isochoric heating for fast ignition

M.H. Key<sup>1</sup>, K. Akli<sup>2</sup>, F. Beg<sup>5</sup>, M.H. Chen<sup>1</sup>, H.-K. Chung<sup>1</sup>, R.R. Freeman<sup>2,3</sup>, M.E. Foord<sup>1</sup>, J.S. Green<sup>6,7</sup>, P. Gu<sup>2</sup>, G. Gregori<sup>1</sup>, H. Habara<sup>8</sup>, S.P. Hatchett<sup>1</sup>, D. Hey<sup>2</sup>, J.M. Hill<sup>2</sup>, J.A. King<sup>2</sup>, R. Kodama<sup>8</sup>, J.A. Koch<sup>1</sup>, K. Lancaster<sup>6</sup>, B.F. Lasinski<sup>1</sup>, B. Langdon<sup>1</sup>, A.J. MacKinnon<sup>1</sup>, C.D. Murphy<sup>6,7</sup>, P.A. Norreys<sup>6</sup>, N. Patel<sup>2</sup>, P. Patel<sup>1</sup>, J. Pasley<sup>5</sup>, R.A. Snavely<sup>1</sup>, R.B. Stephens<sup>4</sup>, C. Stoeckl<sup>10</sup>, M. Tabak<sup>1</sup>, W. Theobald<sup>10</sup>, K. Tanaka<sup>8</sup>, R. Town<sup>1</sup>, S.C. Wilks<sup>1</sup>, T. Yabuuchi<sup>9</sup> and B. Zhang<sup>2</sup>

<sup>1</sup> Lawrence Livermore National Laboratory, Livermore, CA 94550, USA

<sup>2</sup> Department of Applied Sciences, University of California Davis, Davis, CA 95616, USA

<sup>3</sup> Ohio State University, Columbus, Ohio 43210, USA

<sup>4</sup> General Atomics, San Diego, CA 92186, USA

<sup>5</sup> University of California, San Diego, San Diego, CA 92186, USA

<sup>6</sup> Central Laser Facility, CCLRC, Chilton, Didcot OX11 0QX, UK

<sup>7</sup> Blackett Laboratory, Imperial College, London SW7 2AZ, UK

<sup>8</sup> Institute for Laser Engineering, Osaka University, Suita, Osaka, Japan

<sup>9</sup> Graduate School of Engineering, Osaka University, Suita, Osaka, Japan

<sup>10</sup> University of Rochester-Laboratory for Laser Energetics, Rochester, NY 14623, USA

**Abstract.** Isochoric heating by electrons has been measured in the two limiting cases of small area thin foils with dominant refluxing and cone-long-wire geometry with negligible refluxing in the wire. Imaging of Cu K $\alpha$  fluorescence, crystal x-ray spectroscopy of Cu K shell emission, and XUV imaging at 68 eV and 256 eV are discussed. Laser power on target was typically 0.5 PW in 0.7 ps. Heating by focused proton beams generated at the concave inside surface of a hemi-shell and from a sub hemi-shell inside a 30° cone has been studied with the same diagnostic methods plus imaging of proton induced K $\alpha$ . Conversion efficiency to protons has been measured and modeled. Conclusions from the experiments, links to theoretical understanding and relevance to fast ignition are outlined.

### 1. ELECTRON ISOCHORIC HEATING

In cone coupled electron fast ignition, laser generated electrons transport energy and ignite a small hot spot in the compressed fuel. The laser to plasma coupling is via a hollow cone and the energy is transported by relativistic electrons of a few MeV average energy over a distance of the order of 100  $\mu\text{m}$  into DT at about 300  $\text{gcm}^{-3}$  and confined within a diameter <40  $\mu\text{m}$ . The total energy deposited in the hot spot is about 20 kJ in 10 ps. Overall coupling efficiency between laser energy and thermal energy in the ignition hot spot should exceed 10% and preferably reach 20% (as seen in the first small scale integrated experiments [1]) to make the scheme practically attractive.

Studies and modeling of laser accelerated electron sources, the transport of energy by electrons and the consequent isochoric heating have advanced considerably but there is still no well established modeling capability to enable extrapolation from small scale experiments to full scale FI and the processes are complex and challenging from both experimental study and modeling aspects. We have recently used two limiting cases illustrated in figure 1, which address specific issues in electron transport and offer good opportunities for comparison with modeling.

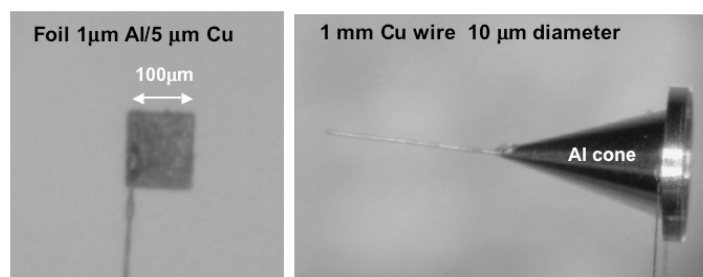


**Figure 1.** The two types of target.

Thin foils of small area constrain electrons to reflux between the surfaces in a time short compared to the laser pulse duration so that there is always approximate cancellation of the net injected current by reflux current, thus eliminating the effect of Ohmic heating by the return current of cold electrons, which is a dominant effect in initially cold solid targets in the absence of refluxing. In the opposite limit a hollow cone couples the laser to a long thin wire and provides a situation where there is complete compensation of the fast electron injection into the wire by the cold electron return current, thus maximum Ohmic effects. The geometry is simple in that the area of the current flow is constant and equal to the cross sectional area of the wire.

The experiments discussed here used the PW laser beam line at the RAL Vulcan laser facility, delivering on target typically 0.5PW, 350J pulses of 0.7ps duration with a peak intensity of  $3 \times 10^{20} \text{ Wcm}^{-2}$  and a pre-pulse of about 1.5 ns duration with an intensity contrast better than  $10^7$ . The diagnostics discussed here are rear side XUV imaging at 68 eV and 256 eV using near normal incidence multi-layer coated spherical mirrors, Highly Ordered Pyrolytic Graphite (HOPG) crystal spectroscopy of K-shell emission from front and rear, and near normal incidence spherical crystal Bragg reflection imaging of Cu  $K\alpha$ .

### 1.1 Low mass thin foil targets

A typical thin foil target experiment used a  $100 \mu\text{m}$  square of Cu,  $5 \mu\text{m}$  thick coated on the irradiated side with  $1 \mu\text{m}$  of Al. In figure 2 the rear side XUV images at 68 eV and 256 eV can be compared and they show how the shorter duration of emission at the higher photon energy freezes the image at the isochorically-heated stage before significant expansion. Clearly seen in the 256 eV image is a  $50 \mu\text{m}$  wide hot spot.

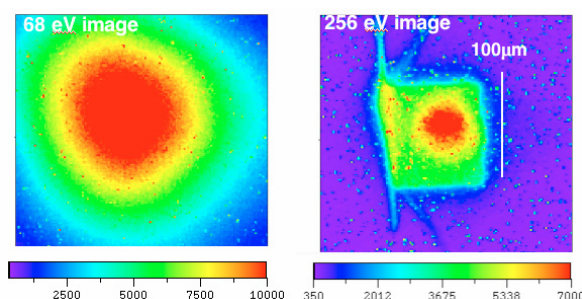


**Figure 2.** 68 eV and 256 eV CCD images of the small area thin foil target, Color bar shows CCD counts.

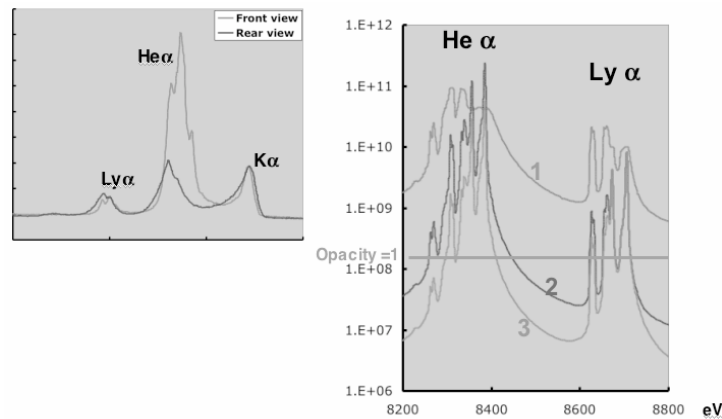


**Figure 3.** Left: the front view and back view HOPG spectra. Right: modeling of the emissivity (2), opacity (3) and opacity corrected emission (1) for 2 keV temperature in  $5\ \mu\text{m}$  of Cu.

Modeling with Lasnex and absolute calibration of the imaged intensity give an estimate of the temperature pattern. The modeling shows that the computed xuv intensity pattern is almost identical whether the initial condition has no axial temperature gradient or half the thickness is at twice the average temperature and half at a low temperature. Thermal conduction by the bulk electrons eliminates the axial temperature variation in a shorter time than the duration of the 256 eV xuv emission (50% of the xuv energy is emitted in  $<50$  ps). Trial patterns of initial temperature were assumed in arriving at the conclusion that the central peak temperature was 2 keV and the temperature at the margins was 500 eV. The thermal energy content was estimated from the fitted temperature pattern via the EOS of Cu and it was 8% of the laser energy.

Cu K shell spectra from the front and back are compared in figure 3 with their intensities normalized to make the  $K\alpha$  emission equal, consistent with the modeled transparency of the source of  $K\alpha$ . Striking in the data is the front to back difference in the  $He\alpha$  and satellite spectrum with 3:1 intensity ratio and reversal of ratios between resonance and satellite lines. This indicates high opacity and a strong axial temperature gradient, the front side being much hotter during the x-ray emission phase (which is much shorter in duration than the xuv emission). The front spectrum was little changed for thicker targets and targets of larger area with or without the  $1\ \mu\text{m}$  over coating of Al. Spectroscopic modeling of emissivity, absorptivity and emission per unit area for a  $5\ \mu\text{m}$  thick homogeneous slab of Cu in steady state LTE also shown in figure 3. It indicates that the observed ratio of  $Ly\alpha$  to  $He\alpha$  is consistent with at least 2 keV temperature and that opacity levels for  $He\alpha$  may reach several 100. Further modeling work is in progress to better understand whether transient effects and temperature gradient effects cause this simple analysis to give an under estimate of the front temperature.

More detailed information on the axial temperature gradient was obtained very recently with layered targets with preliminary results illustrated in figure 4. The total thickness of the targets was  $5\ \mu\text{m}$  and the layers were arranged from front to back with Mo as a coating in front of a  $0.5\ \mu\text{m}$  layer of Ni, a further Mo spacer and a  $1\ \mu\text{m}$  layer of V. The K shell spectra of Ni are shown in figure 4. Mo  $K\alpha$  in 2<sup>nd</sup> order is also seen. The main result is that with no Mo in front of the Ni, there is strong excitation of Ni  $He\alpha$  and significant Ni  $Ly\alpha$  emission. With  $0.5\ \mu\text{m}$  Mo over-coating the thermally excited  $He\alpha$  and  $Ly\alpha$  lines are reduced a factor of 4 and with  $1\ \mu\text{m}$  Mo they are essentially eliminated. The V spectrum in all cases showed only the hot electron excited  $K\alpha$  and no  $He\alpha$  or  $Ly\alpha$ . A preliminary conclusion from these spectra is that a thickness of about  $1\ \mu\text{m}$  reaches a high temperature of about 2 keV and that the rear surface is not heated to more than about 500 eV.

As argued initially cold return current and associated Ohmic heating should be suppressed by refluxing and collisional heating with refluxing is axially uniform. The data suggest however a significant fraction

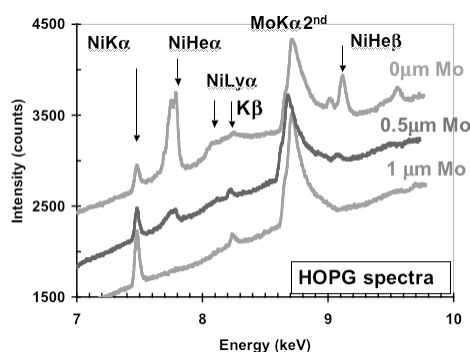


**Figure 4.** HOPG spectra of the layered targets.

of the total thermal energy may initially be deposited in 20% of the target thickness. Some PIC modeling analyses show a surface layer with extremely strong Weibel filamentation, which can enhance Ohmic heating in proportion to the factor by which the current density is increased. In addition the strong azimuthal magnetic field generated in the surface region may trap lower energy electrons and localize their energy deposition. Work is well advanced to develop a hybrid PIC modeling description of these data [2].

## 1.2 Cone wire targets

We discuss here a cone wire target with a  $10\ \mu\text{m}$  diameter Cu wire 1 mm long attached to the tip of a hollow cone of Al  $10\ \mu\text{m}$  thick with  $30^\circ$  cone angle and wall thickness of  $10\ \mu\text{m}$  near its tip. The cone was truncated at  $30\ \mu\text{m}$  diameter with a small hole in which the wire was glued. Figure 5 illustrates the 256 eV xuv image and the HOPG Cu  $K\alpha$  spectrum from this target. The xuv image is dominated by the heated tip region of the cone. The view is oblique as illustrated by the superposed circles. The wire is seen as a weaker emission feature observed only in a  $100\ \mu\text{m}$  region closest to the cone tip. Lasnex modeling of an exploding wire and absolute calibration of the image intensity gives 350 eV as the maximum temperature in the wire. The HOPG spectrum of the  $K\alpha$  emission from the wire exhibits broadening to higher energy due to ionization. Following our previous published method of spectroscopic analysis [3] the temporally and spatially averaged temperature is 160 eV. Most  $K\alpha$  emission occurs where the temperature is highest but the emission occurs at all times during heating from the initially cold state, so that the peak temperature should be about twice the average. On this basis the HOPG data are consistent with the xuv data.

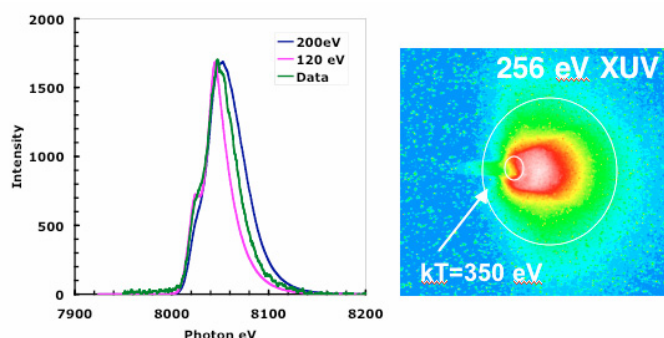


**Figure 5.** Left: HOPG Cu  $K\alpha$  spectrum with model spectra for 200 eV (widest) and 120 eV (narrowest). Right: the 256 eV XUV image of the cone wire target.

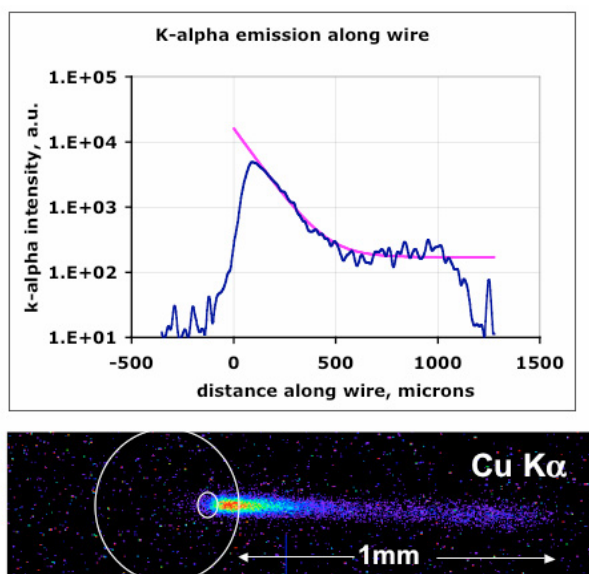


**Figure 6.** The  $K\alpha$  image and intensity line out of the cone wire target.

The imaged  $K\alpha$  emission is shown in figure 6. The intensity falls exponentially from the tip- of the cone with  $100\ \mu\text{m}$  scale length and then remains constant at about 2% of the peak value. The thermal energy in the wire integrating over  $100\ \mu\text{m}$  scale length with a peak temperature of 350 eV, is only 0.8% of the laser energy. Applying a 1D model of inhibition of transport due to the Ohmic potential from the return current [4] for 1 MeV hot electron temperature, a resistivity of  $10^{-6}$  Ohm m (the peak value which occurs at 30 to 100 eV) and requiring a  $100\ \mu\text{m}$  scale length, gives 0.74% of the laser energy entering the wire. There is therefore reasonable consistency between 1D Ohmic inhibition and these observations. Work is in progress modeling this case with the hybrid PIC code LSP and preliminary results agree with the 350 eV peak temperature [2]. There is a non-linearity in the response of the narrow band  $K\alpha$  imager due to the thermal ionization induced broadening and frequency shift of the  $K\alpha$  line. A drop in efficiency of a factor of 0.1 occurs for a peak temperature of 350 eV, indicating that the observed  $100\ \mu\text{m}$  scale length is an overestimate of the scale length of the heating. More complete analysis with LSP will provide simulation of the  $K\alpha$  image including this effect.

## 2. PROTON ISOCHORIC HEATING

### 2.1 Fast ignition concept

Protons offer an alternative means of isochoric heating which has very different physics constraints. The requirement is similar to that for electrons; i.e. to deliver about 15 kJ to  $<40\ \mu\text{m}$  with a proton axial temperature of about 3 MeV. Conversion efficiency to protons should exceed 15% assuming the entire beam is focused to  $<40\ \mu\text{m}$ . Figure 7 illustrates the issues in conceptual full-scale proton fast ignition. The cone must protect the proton source foil from rear surface plasma formation induced by the implosion but it should not cause Moliere scattering outside the required  $<40\ \mu\text{m}$  hot spot. The source foil should be thick enough to protect its rear surface from pre-pulse shock modification but thin enough to allow adiabatic energy loss to acceleration of protons to dominate over collisional energy loss for the refluxing electrons. The laser irradiation should produce sufficiently high temperature electrons uniformly across the source foil to make collisional losses relatively insignificant and to result in a sheath axial development



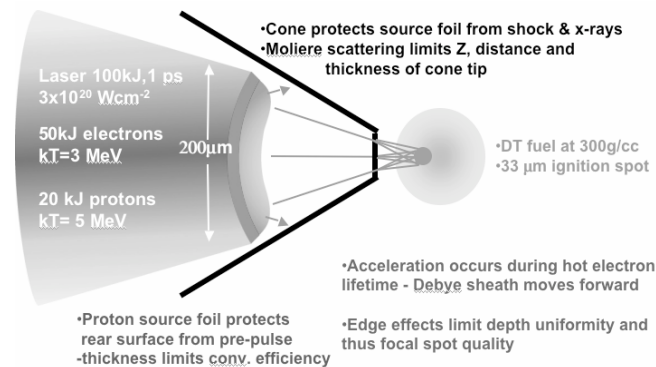


**Figure 7.** Conceptual proton fast ignition.

that is spatially uniform giving radial proton focusing to a spot size  $<40 \mu\text{m}$ . The laser pulse length should be short enough to limit edge effects on the sheath to avoid significant loss of well-focused protons.

## 2.2 Focusing and heating

Following successful initial studies of focusing protons with hemi shell targets, using a 10J, 100 fs laser [5], we extended the study to higher energy and longer pulses PW lasers using the RAL Vulcan and ILE Gekko PW lasers, including the results illustrated in figure 8. The proton focusing is significantly aberrated in these experiments where a relatively small laser focal spot produces a central concentration of electrons and a maximum in the sheath extension giving radial components to the acceleration. We are investigating how to mitigate this using more uniform laser intensity.

In preparation for focusing protons into an imploded plasma we also tested proton focusing using a sub-hemisphere  $20 \mu\text{m}$  thick Al shell inside a  $30^\circ$  cone with detection of the focused protons from Cu

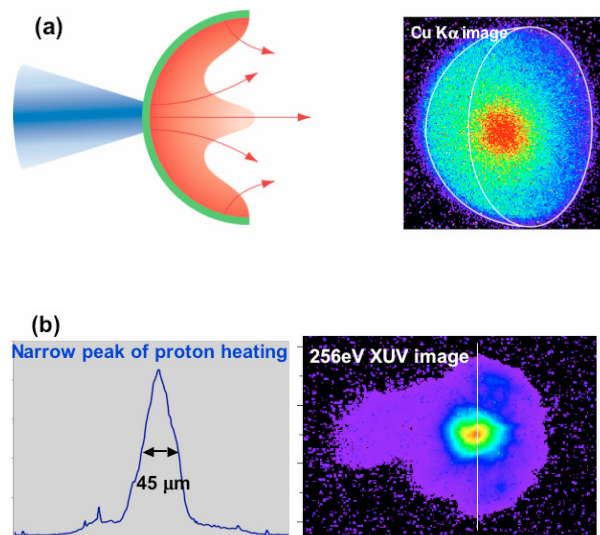


**Figure 8.** (a) Left: schematic sheath and proton plasma flow lines, (a) right:  $K\alpha$  image of  $350 \mu\text{m}$  diameter Cu hemi-shell. (b) 256 eV image of focused proton heating of a polymer foil with associated xuv intensity line out.

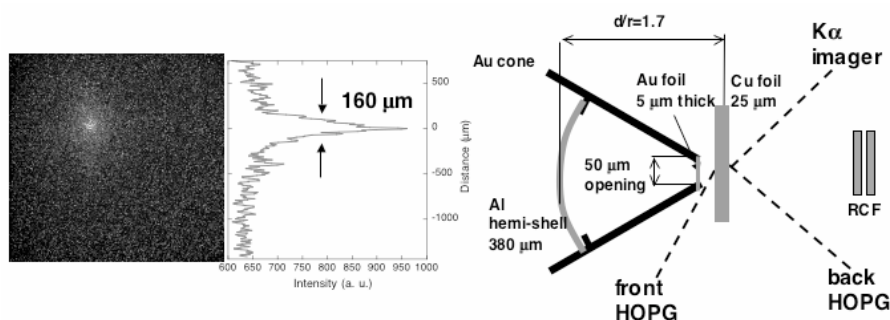


Figure 9. Proton focusing inside a cone. Cu K $\alpha$  image.

K $\alpha$  fluorescence in a 20  $\mu\text{m}$  thick Cu foil as illustrated in very preliminary results shown in figure 9.

The K $\alpha$  image showed the focus to have a fwhm of 160  $\mu\text{m}$  emphasizing the need for better control of the sheath geometry. Comparing front and back HOPG K $\alpha$  spectra there is evidence of greater thermal broadening in the front spectrum consistent with the expected axial variation of proton heating.

### 2.3 Laser to proton energy conversion efficiency

Collected data on conversion efficiency to protons of energy  $>3\text{ MeV}$  are shown in figure 10. The levels achieved do not exceed 10% of the laser energy and optimization of efficiency has not been systematically studied.

We have used, used analytic models and we are developing hybrid PIC modeling to obtain better understanding of how to optimize efficiency for proton fast ignition. From analytic methods it is clear that reflux collisional losses in the foil should be minimized, electron temperature maximized to reduce collisional losses, depletion of the supply of protons should be avoided by providing a sufficiently thick proton rich layer (adsorbed hydrocarbon monolayers are insufficient), and the proton to other ion ratio in the source layer should be as high as possible. An example of 1D numerical modeling with the hybrid PIC code LSP showing  $>50\%$  conversion of electron energy to proton energy is shown in figure 11.

In conclusion, for typically 0.5 PW, 0.7 ps pulses we have studied two limiting cases of electron isochoric heating with and without dominant refluxing and we are using these as benchmark cases for developmental hybrid PIC modeling. We have also measured heating by focused proton beams using both hemi -shell and most recently sub- hemi -shell-in-cone targets. We find that better control of the

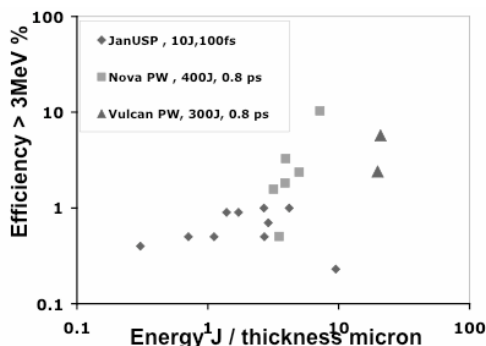
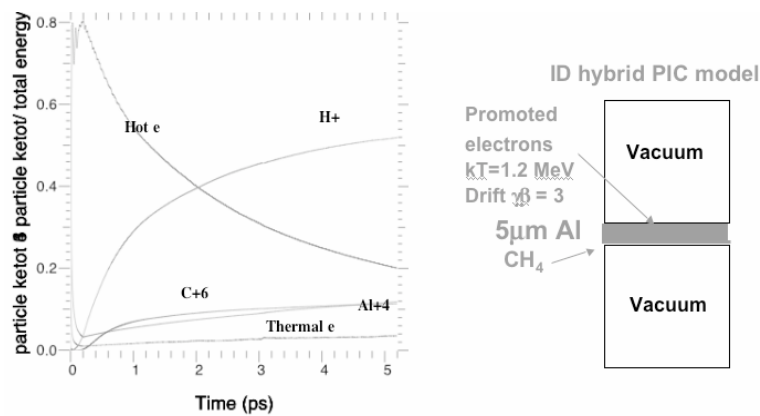


Figure 10. Collected data on conversion efficiency to  $>3\text{ MeV}$  protons versus laser energy/target thickness.





**Figure 11.** Hybrid PIC modeling of time evolution of ion and electron energy fractions in 1D of conversion of hot electron energy in a  $5 \mu\text{m}$  thick Al foil with  $0.1 \mu\text{m}$  of  $\text{CH}_4$  on the rear surface.

accelerating sheath geometry is needed to reduce the focal spot size to that need for FI. Conversion efficiency modeling suggests that efficiencies higher than so far obtained and meeting the need for FI should be possible with suitable design optimization.

### Acknowledgments

We are grateful for the support of the operations staff of the Vulcan and Gekko Laser facilities. This work was performed under the auspices of the U.S. Department of Energy by University of California Lawrence Livermore National Laboratory under contract No. W-7405-Eng-48.

### References

- [1] R K Kodama et al. *Nature*, 418, 933, (2002).
- [2] R Town et al. (*ibid*).
- [3] G Gregori et al. *Contr. Plasma Phys*, 45, 284, (2005).
- [4] A R Bell et al. *Plasma Phys. and Contr. Fusion*, 39, 653, (1997).
- [5] P K Patel et al. *Phys. Rev. Lett.* 91, 125004, (2003).